Earthquakes and Structures, *Vol. 19, No. 3 (2020) 175-188*
DOI: https://doi.org/10.12989/eas.2020.19.3.175

Seismic design and elastic–plastic analysis of the hengda group super high-rise office buildings

Xiaomeng Zhang*, Qingying Ren, Wenting Liu, Songlin Yang and Yilun Zhou

China Architecture Design and Research Group, Beijing 100044, China

(Received April 28, 2020, Revised July 21, 2020, Accepted August 22, 2020)

Abstract. The Hengda Group super high-rise building in Jinan City uses the frame-core tube structural system. With a height of 238.3 m, it is above the B-level height limit of 150 m for buildings within 7-magnitude seismic fortification zones. Therefore, it is necessary to apply performance-based seismic design to this super high-rise building. In this study, response spectrum analysis and comparative analysis of the structure are conducted using two software applications. Moreover, elastic time-history analysis, seismic analysis under an intermediate earthquake, and elastic–plastic time-history analysis under rare earthquakes are performed. Based on the analysis results, corresponding strengthening measures are implemented at weaker structural locations, such as corners, wall ends connected to framed girders, and coupling beams connected to framed girders. The failure mode and failure zone of major stress components of the structure under rare earthquakes are analysed. The conclusions to this research demonstrate that weaker locations and important parts of the structure satisfy the requirements for elastic–plastic deformation in the event of rare earthquakes.

Keywords: high-rise building beyond the cold-specificatio; elastic-plastic analysis; performance-based seismic design; frame-corewall structure; seismic calculation

1. Introduction

Numerous studies on stress analysis and computation algorithms for complicated super high-rise buildings have investigated various structural design and seismic conditions. Celarec and Dolsac (2013) obtained accurate results by considering cognitive uncertainty in the performance assessment of structures, thus enabling a more reliable assessment of seismic risks. Zhou (2019) compared the seismic responses of super high-rise building structures based on different seismic design codes, evaluated the reliability of long-cycle seismic design spectra, and analysed the long-cycle period of vibration of two super high-rise buildings. Additionally, he investigated the maximum displacement at the top of buildings and the maximum seismic shear force on the foundations using the response spectrum and dynamic time-history methods. Celik and Ellingwood (2010) studied the seismic performance of reinforced concrete frames that were designed according to gravity loads in low-seismic areas through the probability nonlinear finite element analysis technique. To evaluate the reliability of long-cycle periods of seismic design spectra, Lu *et al*. (2013) constructed a simplified analysis model of a super high-rise building based on the bending–shearing coupling beam model, and analysed the seismic response demand measurements of structures during different structural base stages. Lu *et al*. (2011) constructed a nonlinear finite element model of Shanghai Tower (632 m), which is the highest building in China, and proposed modelling methods and failure criteria for different structural units. Wang *et al*. (2011) assessed the seismic performance of the Wuhan International Securities Building and calculated the seismic responses of the structure through modal superposition response spectrum analysis and time-history analysis. Wu *et al*. (2017) constructed and analysed NosaCAD and Perform-3D models (which are extensively used in nonlinear analysis) for a super high-rise building with 117 floors. The elastic–plastic time-history analysis of this building was implemented to discuss its seismic behaviour. Fan *et al*. (2009) determined the constitutive relation between the CFT columns and steel components of high-rise buildings, and investigated the finite element relations through a shaking table test. Later, they constructed a finite element model of a high-rise building and numerically simulated its seismic response. Wang *et al*. (2018) carried out elasticity analysis and elastic time-history analysis under frequent earthquakes, examined performance design under intermediate earthquakes, and developed the equivalent elasticity analysis and elastic–plastic time-history analysis under rare earthquakes for a super high-rise building in Guangzhou City using a performance-based seismic design method. Yu *et al*. (2015) compared the response spectrum analyses of structures using two software applications. Specifically, they carried out elastic time-history analysis and yield analysis for intermediate earthquakes and implemented elastic–plastic time-history analysis of the structure. Esam *et al*. (2018), Yao *et al*. (2015) and Yan and Ye (2019) analysed super high-rise buildings with different structures and performance standards for components with varying degrees of importance. They recognised the

*Corresponding author, Ph.D.
E-mail: 155203255@qq.com

Copyright © 2020 Techno-Press, Ltd.
http://www.techno-press.com/journals/was&subpage=7
ISSN: 2092-7614 (Print), 2092-7622 (Online)

Fig. 1 Design sketch of the building

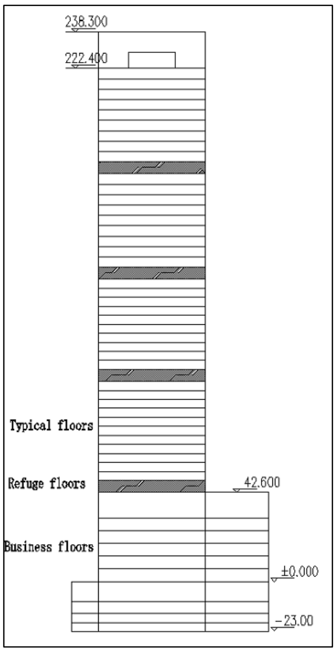

Fig. 2 Profile map of the main building

potentially weak locations and components of the structures under earthquakes, and proposed corresponding seismic strengthening measures. Bagchi *et al*. (2010) described the performance of a 20-story steel structure with a steel frame designed for western Canada. Ali (2016) conducted seismic design for a residence with a 50-story high-rise reinforced concrete structure through elastic response spectrum analysis, and performed a nonlinear time-history analysis using performance-3d to verify its seismic performance with the maximum consideration of earthquake. Taking a 30-story high-rise building as an example, Asgarian *et al*.（2014）studied the performance of a tubular frame as a lateral load-bearing system Simulated and actual (scaled) ground motion records are used to evaluate the dynamic response. In order to put forward some better Suggestions for super high level design, in the United States, especially in California, some extensive studies have been done and working groups were established. Draft regulations (Farzad Naeim 2008) and other documents which includes recommendations on the subject have been developed (Willford *et al* 2008). Moehle (2008) practice- and research-oriented aspects of performance-based seismic design of tall buildings in the United States. Khazaei J (2017) studied the effect of the seismic-soil-structure interaction (SFSI) on the dynamic response of various buildings. Mansouri I (2019) studied the effect of the pulsating characteristics of ground motion on the seismic performance of steel frames. Scholars have conducted various researches and analyses on the seismic design methods (Chikh *et al*. 2017, Li *et al*. 2017, Tsang *et al*. 2018, Lee *et al*. 2018).

The Jinan Hengda Square project is located in the West Railway Station District of Jinan City. The two office buildings (towers D and E) in the south region have, respectively, 32 floors (162.5 m high, with a structure height of 146.8 m) and 50 floors (238.2 m high, with a structure height of about 222.4 m). In this study, we focus the seismic performance of tower E, which consists of four underground floors and 50 overground floors, covering a building area of 99,561 m2. Floors 2-6 house a comprehensive business annex, and the first underground floor houses the business and office hall and the supporting machine room. Underground floors 2-4 include parking lots, civil air defence facilities, and the supporting machine room. A design sketch of tower E is shown in Fig. 1 and a profile map is shown in Fig. 2.

The design life of the project is 50 years. The safety level and fire rating of the building structure are level-2 and level-1, respectively, and the foundation basic design level is A-class. According to the Code for Seismic Design of Building (GB50011-2010, edited in 2016), the seismic grade is 6-magnitude 0.05 g. According to relevant government documents, the whole region must be designed according to 7-magnitude 0.10g. The site-class of the project is classified into III class, and the designed earthquake group is the third groups. According to the relevant table of the Code for Seismic Design of Building (GB50011-2010; edited in 2016), the corresponding characteristic period is 0.65 s. The seismic fortification type is B-class.

2. Structural design

2.1 Model selection for the structural system

The structural system is that of a super high-rise building, and should be evaluated as a reinforced concrete high-rise building taller than B-class height. According to Technical Specification for Concrete Structures of Tall Buildings (JGJ 3-2010), for the frame shear wall structure, when the seismic intensity is 7 degrees 0.1 g, the maximum applicable height for B-class high-rise buildings is 180

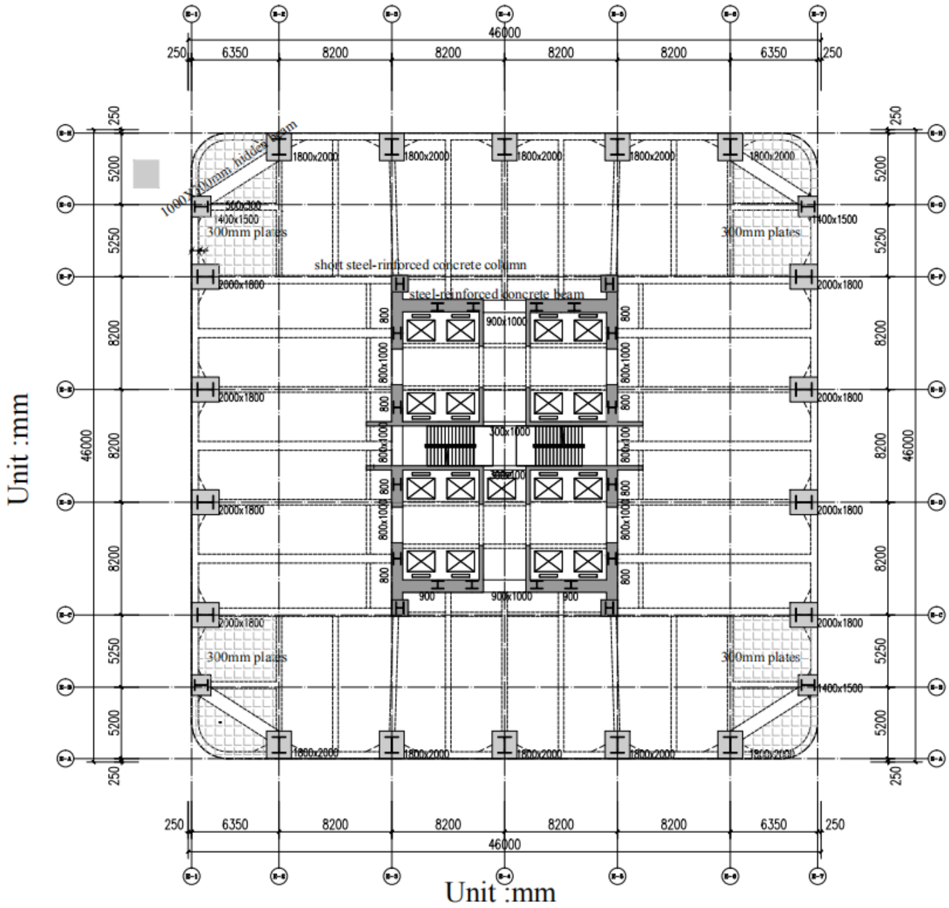

Fig. 3 Layout chart of the structure

meters.

The core tube is in the centre of the tower and is equipped with elevators, an elevator hall, protected stairways, washrooms, and equipment rooms. For buildings reaching the maximum B-class use-height, it is necessary to adopt measures to ensure structural safety and to decrease structural dead loads, seismic effects, and subgrade reactions. Therefore, a wall body constructed from fashioned iron is applied to the bottom strengthening zone of all walls in the core tube of the tower. This improves the seismic properties of the shear wall, decreases the thickness of the wall and the structural dead loads, and increases the structural safety. It also solves the problems of excessive reinforcement of the wall and tensile bottom walls due to elastic behaviour under intermediate earthquakes.

Steel-reinforced concrete columns and steel-reinforced concrete shear walls are the main vertical and lateral force resistant components of the structure. Compared with ordinary reinforced concrete components, steel-reinforced concrete columns allow for a decreased column size and increased usable area, and have excellent fireproof performance; in addition, they increase the ductility of the structure and improve the safety of B-class structures. Moreover, steel-reinforced concrete columns significantly improve the ductility and strength of individual components, without increasing the section area. As a result, structural dead loads are decreased, while the usable area is increased, thus ensuring better quality. Under the premise of building functions, steel-reinforced concrete columns are conducive to developing the role of the surrounding frames, satisfying the requirements for the share ratio of frames, and thereby ensuring sufficient seismic performance of double lateral-resistant structural systems.

The building considered in this study has the following structural characteristics (Fig. 4): (1) Due to the architectural requirements at the corners of the core tube, the frame columns cannot be connected through framed girders. Thus, the corners of the core tube are strengthened by 300 thick plates and 1000 mm × 300 mm hidden beams. (2) The walls at the corners of the core tube bear framed girders from two directions at the same time. There are concentrated stresses in these areas, so short steel-reinforced concrete columns are used for strengthening. (3) The central coupling beam of the core tube is connected with framed girders. The coupling beam is a steel-reinforced concrete beam, which improves the building's seismic performance.

2.2 Determination of basic load value and seismic grade

Considering the main body of the structure and the future preserved loads, the constant load is determined to be 4.0 kN/m2 and the live load is 3.5 kN/m2. The other live

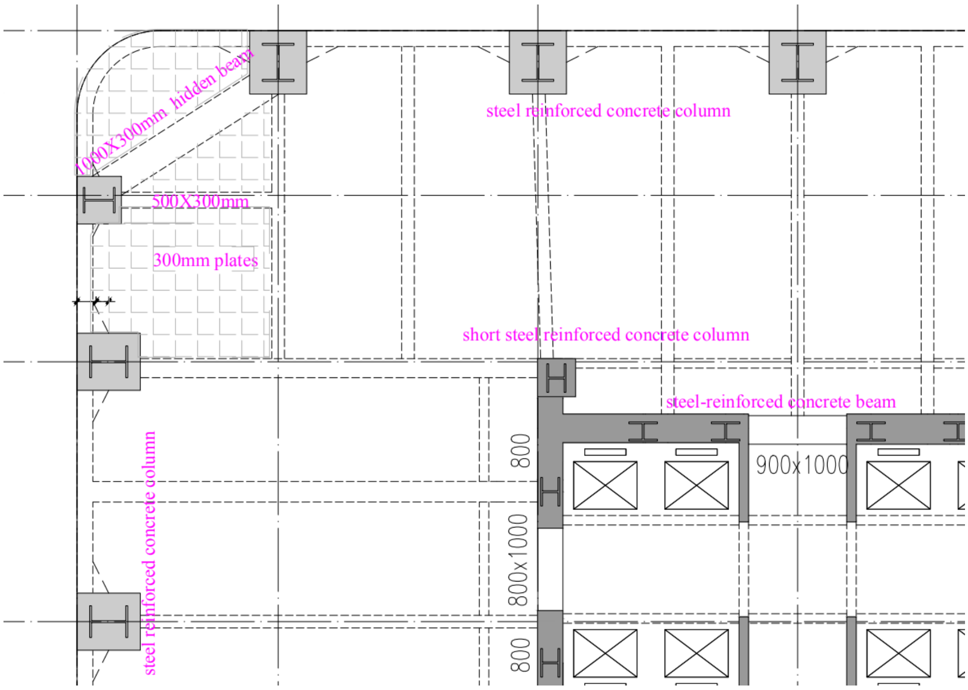

Fig. 4 Schematic diagram of structural characteristics

Table 1 Seismic performance goals

Anti-seismic level		Frequent earthquakes	Medium earthquakes	Rare earthquakes
Limit value of interlayer displacement angle		1/558		1/100
Analysis method		Response spectrum, time-history response analysis	Response spectrum	Response spectrum, dynamic time-history response analysis
Frame column	Shear resistance	Elastic	Elastic	Meet the shear section restrictions
	Bending resistance	Elastic	Non-yield	Several bottom columns yield in bending, no collapse
Coupling beam in seismic shear walls		Elastic	May yield, but retains a certain vertical bearing capacity	May yield, but retains a certain vertical bearing capacity
Coupling beam supporting frame beam		Elastic	Shear resistance in elastic stage, no bending yield	Satisfies shear section restrictions, bending yield
Reinforced area at the bottom of core tube	Shear resistance of wall	Elastic	Elastic	Satisfies shear section restrictions
	Bending resistance of wall	Elastic	Non-yield	Local yield
Other seismic walls		Elastic	Non-yield	Local yield

loads are determined according to the Technical Specification for Concrete Structures of Tall Buildings (JGJ 3-2010): 2.5 kN/m2 in public regions, 3.5 kN/m2 in staircases, 4.0 kN/m2 in refuge storeys, and 7.0 kN/m2 in the elevator room.

2.3 Sections and materials of main structural components

As the structural height increases, the concrete strength grades of the column and shear walls decrease from C70 to C40. The external wall thickness of the shear walls in the core tube decreases from 1000 mm in lower positions to 400 mm in upper positions. The Section of the concrete columns gradually decreases from 2000 mm × 1800 mm in lower positions to 1000 mm × 800 mm in upper positions.

2.4 Performance-based design of the structure

The height of this project is greater than the B-level height limit (180 m) within 7-magnitude regions, as specified by the Technical Regulations on Concrete Structure of High-rise Buildings (JGJ 3-2010). Therefore, the structure requires a performance-based design. The performance of key structural components under different

Table 2 Comparison of main calculation results

		YJK	Midas	limit
Mode of vibration(s)	T1	5.68(X)	5.71	<0.85
	T2	5.04(Y)	5.09	
	T3	4.57(T)	4.61	
	T3/T1	0.81	0.81	
Maximum displacement of vertex (mm)	X-direction wind	154.01	146.8	
	Y-direction wind	105.05	95.3	
	X-direction earthquake	222.23	221.53	
	Y-direction earthquake	181.73	182.18	
Maximum inter-storey displacement angle	X-direction earthquake	1/776 (n=39)	1/782 (n=41)	<1/558
	Y-direction earthquake	1/883 (n=38)	1/892 (n=38)	
Ratio of maximum displacement to average displacement	X-direction earthquake	1.22 (n=1)	1.22 (n=1)	<1.4
	Y-direction earthquake	1.27 (n=2)	1.28 (n=3)	
Basal shear (kN)	X-direction unidirectional earthquake	32058.98 (1.433%)	30701.94 (1.45%)	X≥1.20%
(Shear weight ratio)	Y-direction unidirectional earthquake	33408.58 (1.493%)	31848.13 (1.50%)	Y≥1.20%
Axial pressure ratio	Frame column	0.6	0.56	<0.65
	Shear wall	0.49	0.43	<0.5
Total seismic mass (t)		223775	216061	

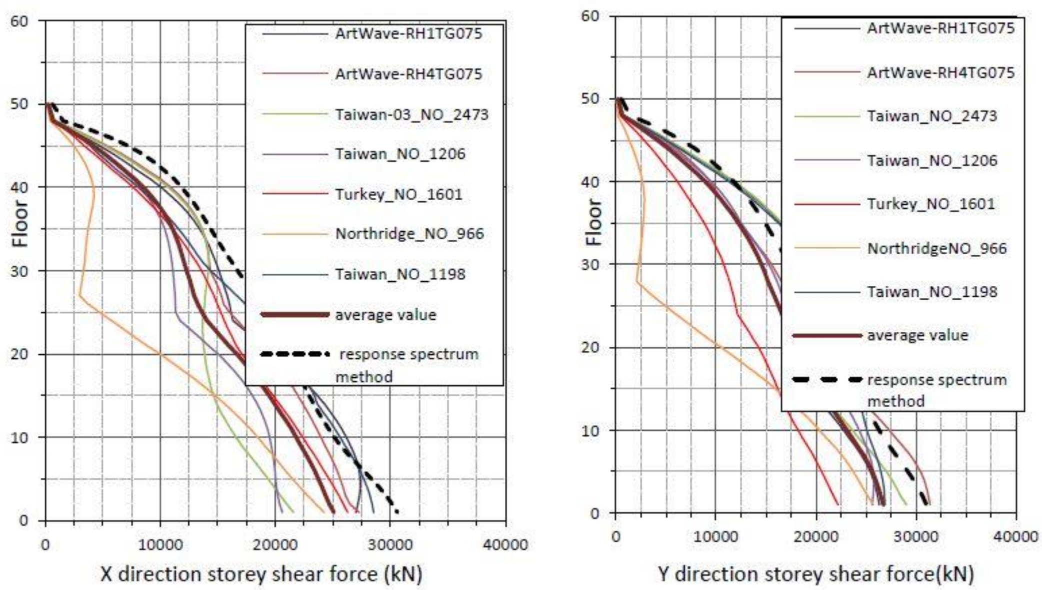

Fig. 5 Storey shear forces

seismic levels are summarised in Table 1.

3. Computational analysis under frequent earthquakes

During the design process, elastic analysis and elastic time-history analysis under frequent earthquakes, yield and elastic analysis under intermediate earthquakes, and elastic–plastic time-history analysis under rare earthquakes were conducted according to the performance goals identified in Table 1.

3.1 Elastic response spectrum analysis under frequent earthquakes

For the elastic response spectrum analysis under frequent earthquakes, the main project indexes were calibrated and compared using YJK and Midas. In the calculation process, response spectrum analysis was applied under consideration of the reverse coupling effect, accidental eccentricity, and two-way seismic effects. The results are presented in Table 2.

Table 2 indicates that that calculation results given by YJK and Midas are broadly consistent. All structural indexes satisfy the requirements of the relevant standards. An analysis of the results leads to the following conclusions:

- The stiffness difference between the structure in any two directions is small. The first reverse cycle/first

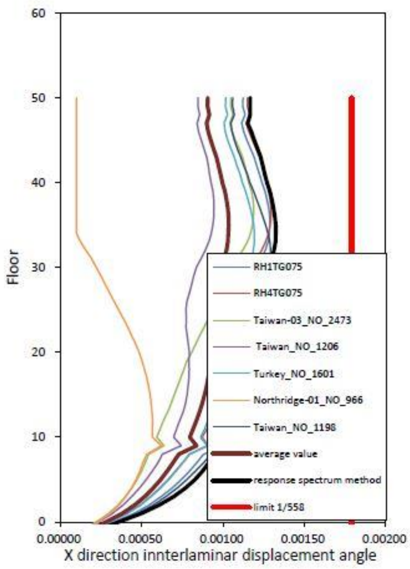

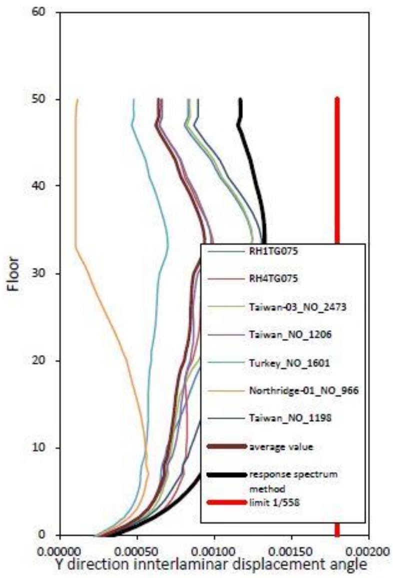

Fig. 6 Interlaminar displacement angle

translation cycle of the structure is less than 0.85, which satisfies the requirements of the relevant standards.

• The shear-weight ratio in two directions at the bottom of the structure satisfies the requirement of being no less than 1.2% in the Design Code for Seismic Structure.

• The maximum storey drifts of the structure in two directions are both smaller than the limit in the norms (1/558). With consideration of accidental eccentricity, the YJK results reflect that the maximum floor displacement/average displacement (maximum storey drift/average storey drift) is 1.28, which satisfies the requirements of the relevant standards (i.e., <1.4).

3.2 Elastic time-history analysis under frequent earthquakes

To make a supplementary analysis of the response spectrum, an elastic time-history analysis of the project under frequent earthquakes was carried out using YJK. Five groups of natural waves and two groups of artificial waves on the III-type site were chosen for the elastic time-history analysis. This project considered two-way horizontal seismic effects and found the acceleration peak ratio of seismic waves along the principle and secondary directions to be 1:0.85.

The elastic time-history analysis results were compared with the calculated results using the mode-superposition response spectrum method. The comparison results are shown in Figs. 3 and 4. The base shear under the effect of seismic waves is smaller than that in the response spectrum method. This means that the results calculated using the response spectrum analysis method are applicable to the design of this structure. Additionally, the interlaminar displacement angle under the effect of seismic waves is smaller than that given by response spectrum analysis, and the interlaminar displacement angle curve exhibits no sudden changes. The lateral rigidity of the structure changes uniformly with height, though again there are no sudden changes. However, under the action of different seismic waves, the response of the structure changes greatly, and the seismic wave 996 in this project has a large deviation from other waves, which can be ignored.

3.3 Elastic analysis under intermediate earthquakes and yield analysis under rare earthquakes

3.3.1 Shear elasticity analysis of the bottom shear wall under intermediate earthquakes

Under intermediate earthquakes, the shear wall and frame columns must satisfy certain seismic performance requirements in terms of shear elasticity. When performing elastic analysis under intermediate earthquakes, the maximum seismic influence coefficient is adjusted to 2.8 times that under frequent earthquakes. The seismic grade of the components runs on a four-level scale. According to the analysis results for the shear pressure ratio under intermediate earthquakes (see Fig. 7), shearing sections in most regions of the shear walls and frame columns satisfy the requirements of the relevant standards. Reinforcement of the shear wall columns in the shear mutation floor during the construction stage can satisfy the stress requirements under intermediate earthquakes. Horizontal reinforcement of the shearing wall and frame columns under the elasticity effect of intermediate earthquakes, as well as the vertical reinforcement of the shearing wall and frame columns under the unyielding effect of intermediate earthquakes, were analysed. It was found that most reinforcements in the shearing wall and frame columns are detailing reinforcement. Only a few edge members have any reinforcement, but this increases the seismic elasticity. Under intermediate earthquakes, the vertical components all satisfy the seismic performance goal of not yielding upon bending stress and shear modulus. The bearing capacity of edge regions with significant bottom reinforcement is

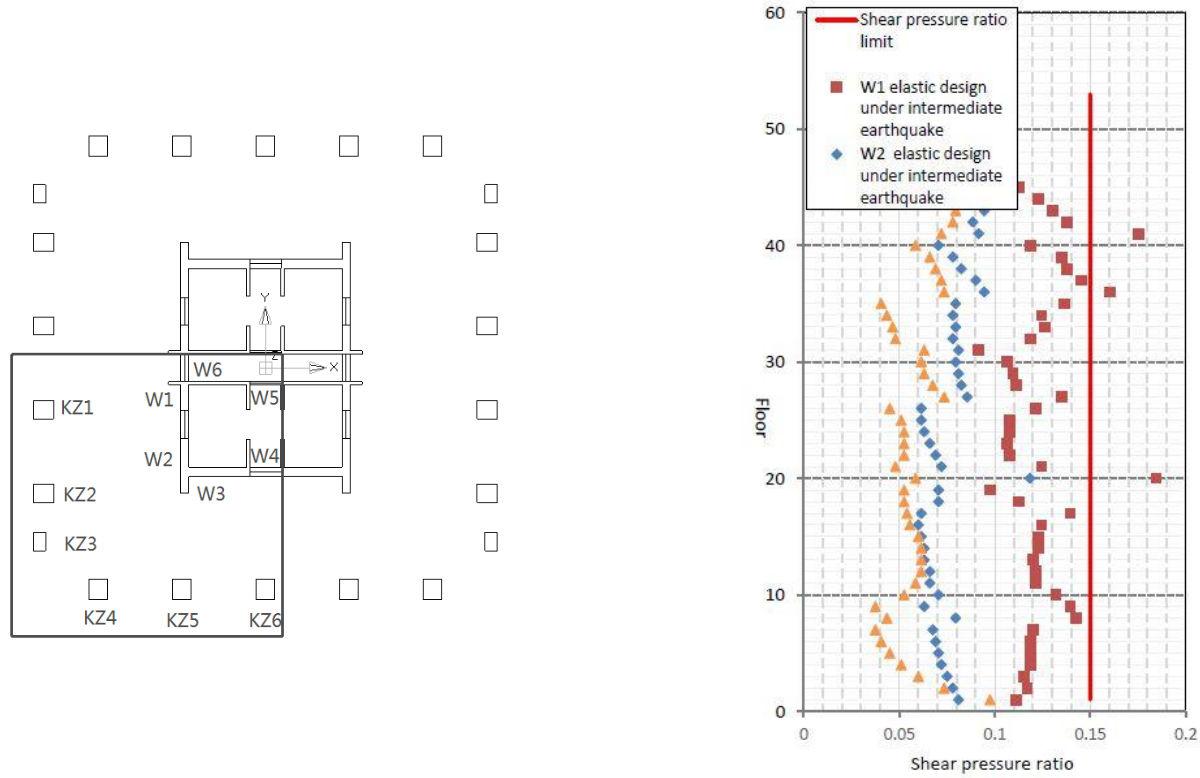

Numbers of shearing wall columns in the bottom reinforcement region

Shear pressure ratio of a typical shearing wall

Fig. 7 Shearing wall and shear pressure ratio of frame columns

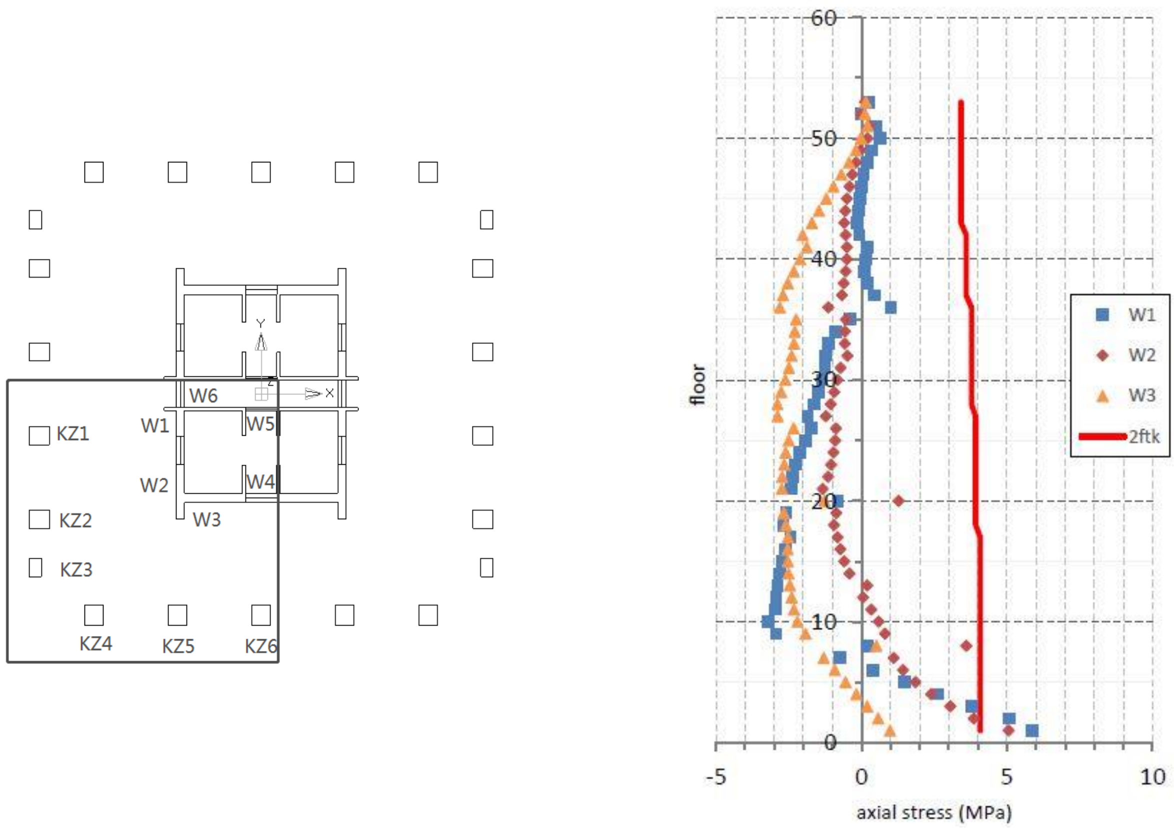

(a) Numbers of frame columns and shearing walls

(b) Changes of axial tensile stress of shearing walls

Fig. 8 Variation in the tensile stress of shearing walls

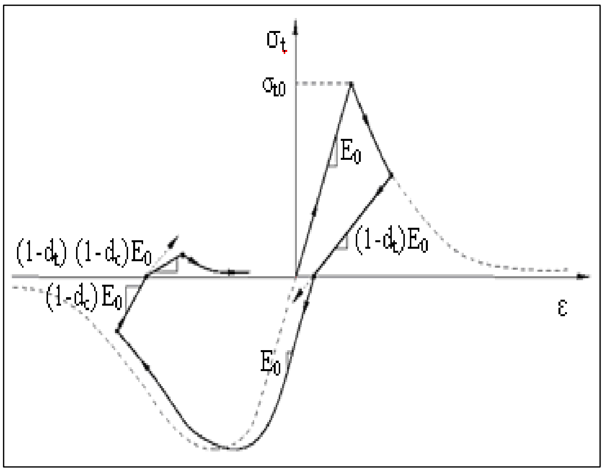

(a) Hysteresis curve of concrete

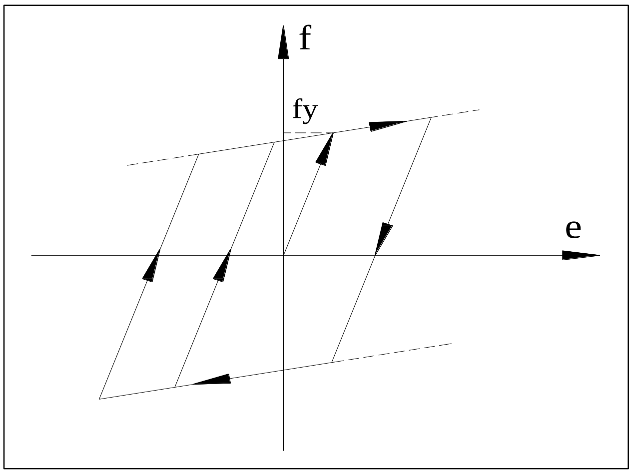

(b) Multilinear kinematic hardening model of double broken line of steel and rebar

Fig. 9 Constitutive model of materials

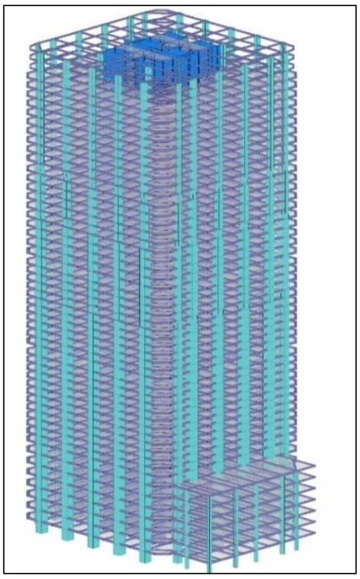

Fig. 10 SAUSAGE model of the tower

satisfied by using fashioned irons.

3.3.2 Eccentric tension analysis of shearing wall

To investigate the tension behaviour of the edges of the wall column under intermediate earthquakes, the tensile stresses of the shear walls of the whole building were analysed. The results in Fig. 8 indicate that some wall columns exhibit tensile stresses, although most floors are never subjected to tensile forces more than twice the standard value of concrete tensile strength. There is significant eccentric tension at the end walls of some floors and the comprehensive wall columns are in tension. Fashioned irons placed at the corners of shearing walls receive all of the tensile forces generated by unyielding wall columns under intermediate earthquakes. The fashioned irons extend along the height of the building until the tensile stress is less than the standard value of concrete tensile strength under unyielding conditions of intermediate earthquakes.

3.3.3 Main structural countermeasures for ultralimit height

Countermeasures for the ultralimit height include the following:

• Enhance the frame as the second defensive line and reinforce the frame columns appropriately.
• Add steel ribs to the frame columns of the bottom floors to increase structural ductility.
• Constrain the edge components at the bottom reinforcement position when the axial pressure ratio of the shearing wall is greater than 0.10. Constrain the edge components at other positions when the axial pressure ratio of the shearing wall is greater than 0.25.
• Optimise components to relieve structural dead loads.
• Equip the bottom strengthening region of the core tube and the upper floors with fashioned irons to ensure that no yielding occurs upon bending under intermediate earthquakes.

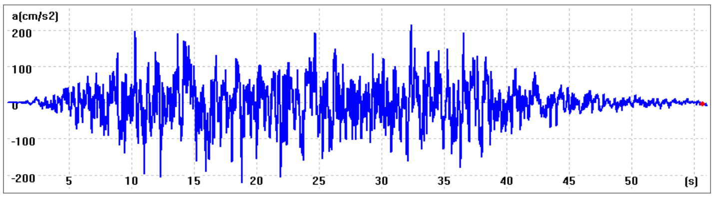

(a) The main direction of L770-1 seismic waves

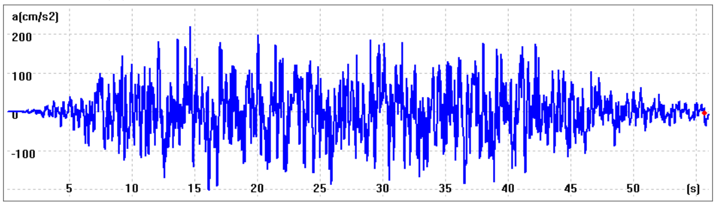

(b) The secondary direction of L770-1 seismic waves

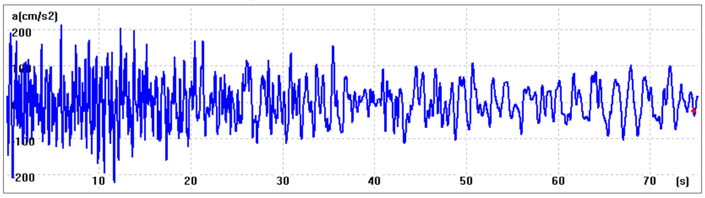

(c) The main direction of L0802 seismic waves

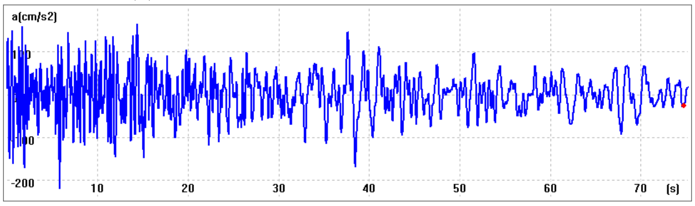

(d) The secondary direction of L0802 seismic waves

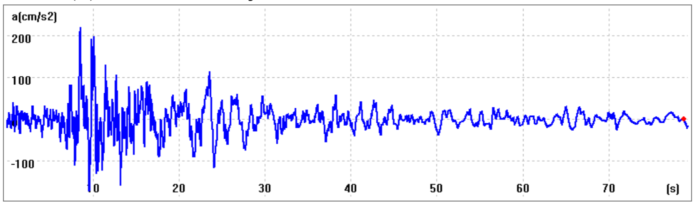

(e) The main direction of L0058 seismic waves

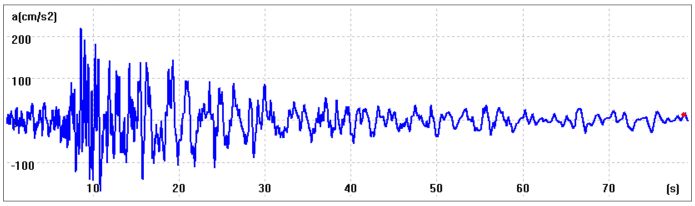

(f) The secondary direction of L0058 seismic waves

Fig. 11 Time history curve of seismic waves

• Determine the minimum reinforcement requirements of various structural equipment; these will be slightly higher than the relevant standards.

4. Elastic–plastic dynamic time-history analysis under rare earthquakes

4.1 Constitutive model and unit model in elastic time-history analysis

To realise the seismic performance goal of "no collapse under rare earthquakes", elastic–plastic dynamic time-history analysis under rare earthquakes was conducted using the SAUSAGE (Wang *et al*. 2012) software.

4.1.1Constitutive model of materials

Considering the tensile strength difference of concrete materials and the rigidity and strength degeneration and recovery over tensile and compressive cycles, the standard values of axial compression and axial tensile strength and the constitutive relation curve of concrete were determined according to Appendix C of the Design Code for Concrete

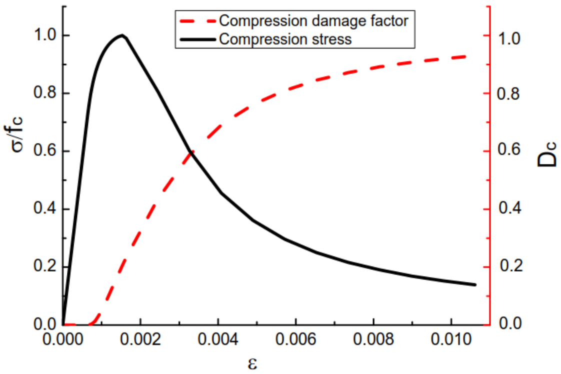

Fig. 12 The relation diagram between damage factor and stress-strain curve of concrete

Structure (GB50010) (see Fig. 9(a)). The double broken line model was applied to both steel and rebar in a reinforcement segment. The Bauschinger effect under tension–compression cycles was also considered, and no rigidity degeneration was observed in the circulation process (see Fig. 9(b). Values of the ultimate intensity and yield intensity of steel were determined according to the Design Code for Concrete Structure (GB50010).

4.1.2 Unit model of components in SAUSAGE

Beams, columns, and inclined struts were simulated as Timoshenko beam units, which have shearing deformation rigidity, whereas the corners and displacement were interpolated independently. The fibre beam model was used to account for the elastic–plastic stress characteristics of the beam units. Each section of a beam unit is composed of concrete, rebar, and one or several steel materials. During fibre division, the concrete, rebar, and steel are meshed independently, and the shearing wall, coupling beam, and floor are simulated by shell units, which behave like corners under deformation. A hierarchical shell model was used to account for the elastic–plastic stress features of the shell unit. Each shell unit can be divided into multiple layers of concrete and multiple layers of distributed rebar along the thickness direction. When calculating the internal force of a shell unit, the strain and stress of each layer of concrete or rebar are calculated according to the plane cross-section assumption. Secondly, integration along the thickness gives the generalised internal forces along the thickness direction. Finally, integration at each Gauss integral point gives the internal force of the shell units.

4.2 Overall calculation results

The elastic–plastic analysis model was used to calculate the reinforcement required for performance design under frequent earthquakes, intermediate earthquakes, and rare earthquakes. Reinforcement was determined to be required when the structural calculation returned a higher value than that needed for standard construction. The calculation model only considers the overground structure (Fig. 10). Two groups of strong earthquake records and one group of artificial simulated earthquake waves were chosen for

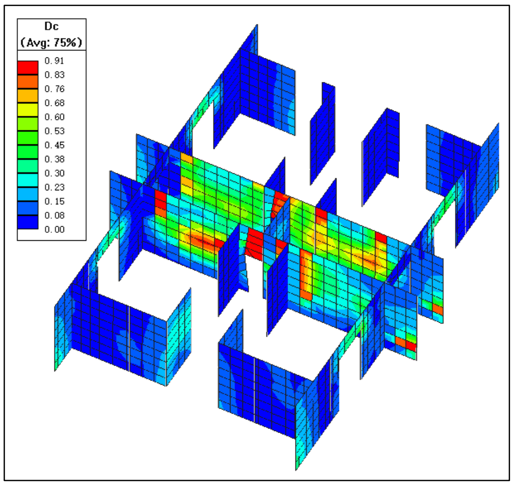

(a) Damage distribution on the first-floor shearing wall

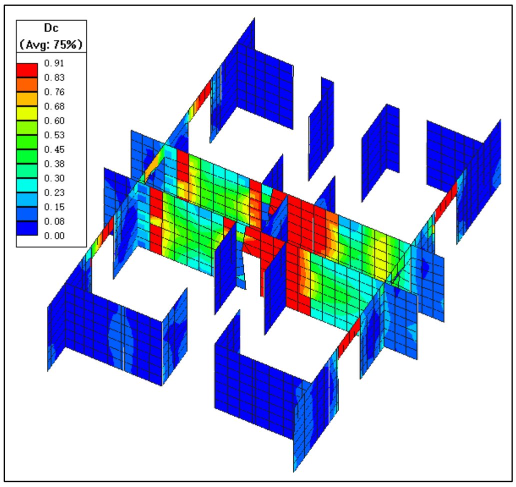

(b) Damage distribution on the third-floor shearing wall

Fig. 13 Damage distribution on walls

analysis (Fig. 11). Table 3 indicates that the interlaminar displacement angle along the X direction is 1/133 and the maximum interlaminar displacement angle along the Y direction is 1/132. Both of these values are within the limits of seismic performance (1/100).

4.3 Elastic–plastic seismic performance analysis

The earthquake wave USER1(L770-1), which leads to the maximum seismic response, was used to analyse the seismic performance of components

4.3.1 Seismic performance analysis of shearing walls

The damage to the shearing walls of the whole building was analysed. The compressive damage distribution of the shearing walls is shown in Fig. 13. Coupling beams were formed by placing holes at reasonable locations along the shearing walls, which suffered evident damage and were subjected to significant energies under rare earthquakes. This protects load bearing wall columns and most shearing wall columns on the external surfaces of the core tube, which suffered no damage. There is some compressive damage to edge components at the corners of the local

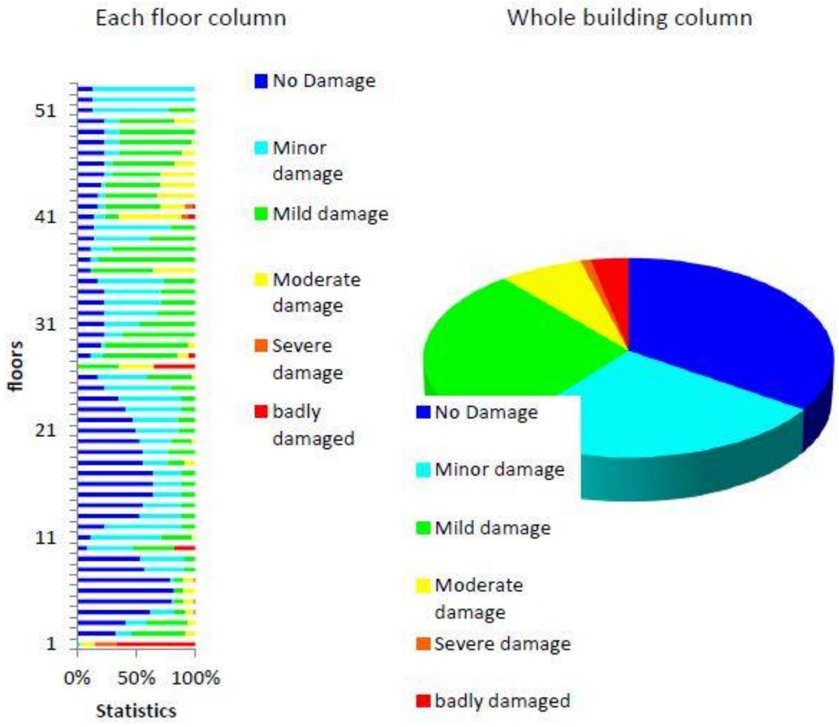

Fig. 14 Statistics on column performance

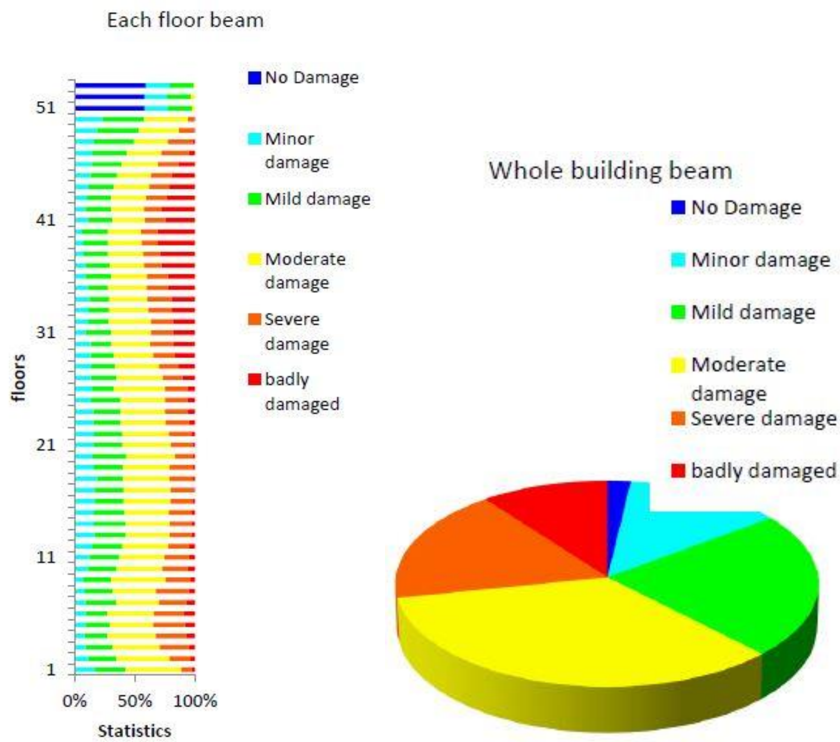

Fig. 15 Statistics on performance of energy-consuming components

bottom shearing walls. However, the maximum damage factor (D_c) is less than 0.2 and the damage width is less than 25% (Fig. 12). When the damage factor is between 0.1 and 0.5 and the damage width is less than 50% of the cross-section width, the wall is defined as moderately damaged. There is local damage to the 300-mm-thick shearing wall at the connections with the core tube. Overall, most shearing walls develop little or no damage, thus satisfying the performance goal.

4.3.2 Seismic performance analysis of frame columns

The compressive damage distribution of the frame

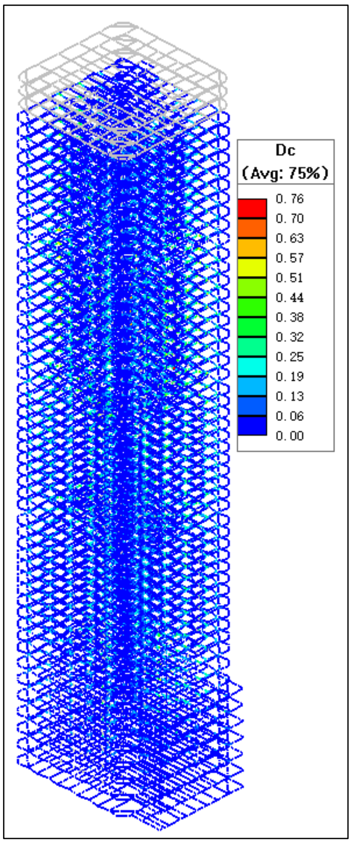

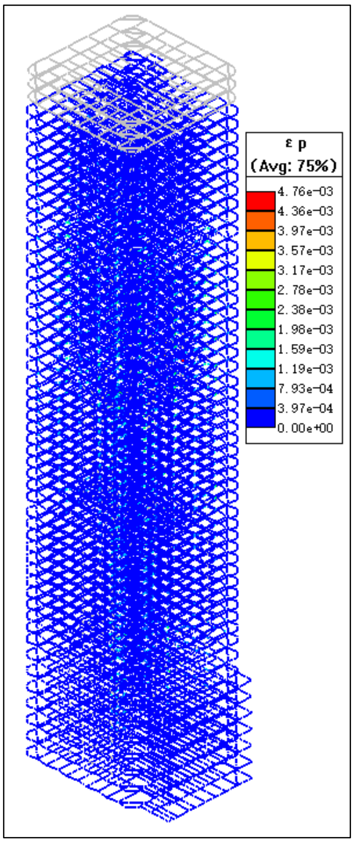

Fig. 16 Compressive damage to concrete beams and plastic strain distribution of rebar

columns is shown in Fig. 14. Mild and moderate compressive damage can be observed in the frame columns of the annex and on several floors, although severe damage is extremely rare. The whole structure has enough seismic bearing capacity and some residual bearing capacity under rare earthquakes. The structure satisfies the preset seismic performance targets.

4.3.3 Seismic performance analysis of energy-consuming components

The compressive damage distribution of the framed girder concrete and the plastic strain distribution on rebar are shown in Figs. 15 and 16. The damage factor(D_c) of some framed girder concrete reached 0.76 and the plastic strain of rebar reached 0.00476(Fig. 12). Most framed girders developed minor, mild, or moderate damage. Some framed girder ends exhibit moderate concrete compressive damage and plastic strain on the rebar. As the framed girder can redistribute internal plastic forces, the overall structure has retained its seismic bearing capacity.

According to the calculation results for elastic–plastic behaviour under rare earthquakes, no plastic strain occurs at the shearing wall (external surface) of the bottom reinforcement region or the vertical rebar of the frame columns. This indicates that the flexural strength of the shearing walls and frame columns in the bottom reinforcement regions satisfies the unyielding requirement for rare earthquakes. The shearing walls and frame columns in the other regions satisfy the performance goal of some bending yield. The coupling beam develops evident damage and is subjected to significant energies. The framed girder also partially enters the yield stage, thus consuming some degree of energy. However, it is not enough to cause local collapse and endanger the whole structural safety. Thus, the structure will not “collapse under rare earthquakes”.

5. Conclusions

- An anti-earthquake analysis was carried out in this paper for a complex super high-rise building over 200 m in height. Due to high requirements for the use functions of the building in this project, wall thickness, column section and beam height were quite restricted. A composite structural system with steel reinforced concrete member being the main stress-bearing member was proposed in this project. Relative to ordinary super high-rise buildings, the large number of steel reinforced concrete columns inside core tube and frame column could not only reduce sectional dimensions of wall column and structural dead weight but also effectively strengthen mechanical properties of wall column under earthquake. Moreover, the wall body with built-in profile steel effectively bore large tensile stress under frequent earthquake, the ductility of the set circumferential steel reinforced concrete columns was strengthened, and the second safety guarantee was formed by giving full play to circumferential frames.
- Steel reinforced concrete members were set in key stress area to strengthen the whole structure, e.g.,

coupling beams realizing lap joint with frame beams inside core tube and wall body stretching out at the corner of core tube, and seismic performance of the members could be improved greatly. During frequent and rare earthquake analysis, these critical members had to sustain large load and seismic force. After profile steel was arranged, the seismic performance could be satisfied under frequent earthquake. The compressive damage of concrete was less and seismic bearing capacity was greatly enhanced under rare earthquake.

• This project is a super high-rise building with multiple indexes exceeding their respective limits. Various uncertainties existed in the seismic analysis. The error of mode- superposition response spectrum method under complex irregular and long-periodic structure could be avoided through a supplemental analysis of elastic time history. Based on analytical comparison in this project, it could be obtained that for this project, a relatively regular super high-rise building, the result calculated by mode-superposition response spectrum method was relatively conservative and safer than that calculated by elastic time history analysis, and furthermore, the mode-superposition response spectrum method reserved enough redundancy for the structure.

• For the complex super high-rise building, a comparative analysis of two software was implemented, so as to avoid possible error in the software design process and ensure that the seismic design of this project could satisfy the structural requirements for bearing capacity, overall stability, structural lateral load resistance and deformation control.

• A structural analysis of critical vertical members under frequent earthquake elasticity was carried out, and the analysis results showed that tensile resistance, shear resistance and compression resistance of critical structural members could be strengthened through strengthening measures like strengthening horizontal reinforcements between wall body and column and setting profile steel inside wall body and columns, and moreover, this could ensure that the main stress-bearing members in the structure were still under elastic phase under frequent earthquake.

• The elastic-plastic time history analysis under rare earthquake was carried out to investigate the failure mode and failure mechanism of shear wall, column and beam. The seismic performance of vertical members could be strengthened by setting profile steel in shear wall and column, so as to ensure that critical vertical members in the whole structure would not undergo any failure while members like coupling beam and frame beam entered yield state first. Through plastic internal force redistribution, this could exert energy dissipation effect, but not lead to local collapse or endanger the overall structural safety, so the overall earthquake fortification goal could be reached.

References

Asgarian, B., Nojoumi, R.M. and Alanjari, P. (2014), “Performance-based evaluation of tall buildings using advanced intensity measures (case study: 30-story steel structure with framed-tube system)”, *Struct. Des. Tall Spec. Build.*, **23**(2), 81-93. https://doi.org/10.1002/tal.1023.

Bagchi, Y.A.A. (2010), “Seismic performance of a 20-story steel-frame building in Canada”, *Struct. Des. Tall Spec. Build.*, **19**(8), 901-921. https://doi.org/10.1002/tal.517.

Celarec, D. and Dolšek, M. (2013), “The impact of modelling uncertainties on the seismic performance assessment of reinforced concrete frame buildings”, *Eng. Struct.*, **52**, 340-354. https://doi.org/10.1016/j.engstruct.2013.02.036.

Celik, O.C. and Ellingwood, B.R. (2010), “Seismic fragilities for non-ductile reinforced concrete frames-Role of aleatoric and epistemic uncertainties”, *Struct. Safety*, **32**(1), 1-12. https://doi.org/10.1016/j.strusafe.2009.04.003.

Chikh, B., Mebarki, A., Laouami, N., Leblouba, M., Mehani, Y., Hadid, M. and Benouar, D. (2017), “Seismic structural demands and inelastic deformation ratios: a theoretical approach”, *Earthq. Struct.*, **12**(4), 397-407. https://doi.org/10.12989/eas.2017.12.4.397.

CMC. (2010), Code for design of concrete structures (GB50010-2010).

CMC. (2010), Code for seismic design of buildings (GB 50011-2010).

CMC. (2010), Technical specification for concrete structures of tall building (JGJ 3-2010).

CMC. (2012), GB50009-2012. Load code for the design of building structures. GB50009-2012.

Esam, A. and Yue, S. (2018), “Structural design on super-tall office building for Hubei Branch of Bank of China”, *Build. Struct.*, **2018**(21), 25-30.

Fan, H., Li, Q.S., Tuan, A.Y. and Xu, L. (2009), “Seismic analysis of the world’s tallest building”, *J. Construct. Steel Res.* **65**(5), 1206-1215. https://doi.org/10.1016/j.jcsr.2008.10.005.

Khazaei, J., Amiri, A. and Khalilpour, M. (2017), “Seismic evaluation of soil-foundation-structure interaction: Direct and Cone model”, *Earthq. Struct.*, **12**(2), 251-262. https://doi.org/10.12989/eas.2017.12.2.251.

LATBSDC (2008), “An alternative procedure for seismic analysis and design of tall buildings located in the Los Angeles region”, Berkeley: University of California (PEER Report No. 2010/05).

Lee, H.S. and Jeong, K.H. (2018), “Performance-based earthquake engineering in a lower-seismicity region: South Korea”, *Earthq. Struct.*, **15**(1), 45-65. https://doi.org/10.12989/eas.2018.15.1.045.

Li, S., Tian, J.B. and Liu, Y.H. (2017), “Performance-based seismic design of eccentrically braced steel frames using target drift and failure mode”, *Earthq. Struct.*, **13**(5), 443-454. https://doi.org/10.12989/eas.2017.13.5.443.

Lu, X., Lu, X., Guan, H. and Ye, L. (2013), “Comparison and selection of ground motion intensity measures for seismic design of super high-rise buildings”, *Advan. Struct. Eng.*, **16**(7), 1249-1262. https://doi.org/10.1260/1369-4332.16.7.1249.

Lu, X., Lu, X., Zhang, W. and Ye, L. (2011), “Collapse simulation of a super high-rise building subjected to extremely strong earthquakes”, *Science China Technological Sciences*, **54**(10), 2549.

Mansouri, I., Shahbazi, S., Hu, J.W. and Moghaddam, S.A. (2019), “Effects of pulse-like nature of forward directivity ground motions on the seismic behavior of steel moment frames”, *Earthq. Struct.*, **17**(1), 1-15. https://doi.org/10.12989/eas.2019.17.1.001.

Moehle, J.P. (2008). “Performance-based seismic design of tall buildings in the US”, *In the 14th World Conference on Earthquake Engineering (CD)*, Beijing, China.

Özuygur, A.R. (2016), “Performance-based seismic design of an irregular tall building - a case study”, *Struct.*, **5**, 112-122. https://doi.org/10.1016/j.istruc.2015.10.001.

Tsang, H.H. (2018), "Recommended seismic performance requirements for building structures in Hong Kong", *Earthq. Struct*., **15**(1), 9-17. https://doi.org/10.12989/eas.2018.15.1.009.

Wang, W., Li, B. and Han, J. (2018), "Structural design on super high-rise tower building in Guangzhou Pazhou", *Build. Struct*., **2018**(11), 17-22.

Wang, X. and Li, Z. (2012), "Methods and application of dynamic elastoplastic time history analysis on SAUSAGE software", *Build. Struct*., **2012**(S2), 7-11.

Wang, Y., Zhou, H., Shi, Y., Huang, Y., Shi, G. and Wen, S. (2011), "Seismic analysis of a super high-rise steel structure with horizontal strengthened storeys", *Front. Architect. Civil Eng. China*, **5**(3), 394. https://doi.org/10.1007/s11709-011-0116-8.

Wu, X., Li, Y. and Zhang, Y. (2017), "Elasto-plastic time history analysis of a 117-story high structure", Comput. Concrete, **19**(1), 7-17. https://doi.org/ 10.12989/cac.2017.19.1.007.

Yan, S. and Ye, Y. (2019), "Structural design of Bravo Global Trade Center Tower", Build. Struct., **2019**(13), 30-34.

Yao, Q. and Zhang, C. (2015), "Structural system selection and out-of-code analysis of B block super high-rise building of Glory City in Haikou", Build. Struct., **2015**(18), 41-46.

Yu, J. and Li, L. (2015), "Structural design of super high-rise building of Tianjin Junlin Building", *Build. Struct*., **2015**(1), 1-4.

Zhou, J. (2019), "Comparison of the earthquake response of super-high-rise structures based on different seismic design spectra", *J. Eng. Res*., **7**(4).

AT